Multiplex Serum Cytokine Immunoassay Using Nanoplasmonic Biosensor Microarrays

Pengyu Chen,[†] Meng Ting Chung,[†] Walker McHugh,[‡] Robert Nidetz,[†] Yuwei Li,[†] Jianping Fu,[†,§] Timothy T. Cornell,[‡] Thomas P. Shanley,[‡] and Katsuo Kurabayashi*[,†,⊥]

[†]Department of Mechanical Engineering, University of Michigan, Ann Arbor, Michigan 48109, United States, [‡]Department of Pediatrics and Communicable Diseases, University of Michigan, Ann Arbor, Michigan 48109, United States, [§]Department of Biomedical Engineering, University of Michigan, Ann Arbor, Michigan 48109, United States, and [⊥]Department of Electrical Engineering and Computer Science, University of Michigan, Ann Arbor, Michigan 48109, United States

ABSTRACT Precise monitoring of the rapidly changing immune status during the course of a disease requires multiplex analysis of cytokines from frequently sampled human blood. However, the current lack of rapid, multiplex, and low volume assays makes immune monitoring for clinical decision-making (*e.g.*, critically ill patients) impractical. Without such assays, immune monitoring is even virtually impossible for infants and neonates with infectious diseases and/or immune mediated disorders as access to their blood in large quantities is prohibited. Localized surface plasmon resonance (LSPR)-based microfluidic optical biosensing is a promising approach to fill this technical gap as it could potentially permit real-time refractometric detection of biomolecular binding on a metallic nanoparticle surface and sensor miniaturization, both leading to rapid and sample-sparing analyte analysis. Despite this promise, practical implementation of such a microfluidic assay for cytokine biomarker detection in serum samples has not been established primarily due to the limited sensitivity of LSPR biosensing. Here, we developed a high-throughput, label-free, multiarrayed LSPR optical biosensor device with 480 nanoplasmonic sensing spots in microfluidic channel arrays and demonstrated parallel multiplex immunoassays of six cytokines in a complex serum matrix on a single device chip while overcoming technical limitations. The device was fabricated using easy-to-implement, one-step microfluidic patterning and antibody conjugation of gold nanorods (AuNRs). When scanning the scattering light intensity across the microarrays of AuNR ensembles with dark-field imaging optics, our LSPR biosensing technique allowed for high-sensitivity quantitative cytokine measurements at concentrations down to 5−20 pg/mL from a 1 μL serum sample. Using the nanoplasmonic biosensor microarray device, we demonstrated the ability to monitor the inflammatory responses of infants following cardiopulmonary bypass (CPB) surgery through tracking the time-course variations of their serum cytokines. The whole parallel on-chip assays, which involved the loading, incubation, and washing of samples and reagents, and 10-fold replicated multianalyte detection for each sample using the entire biosensor arrays, were completed within 40 min.

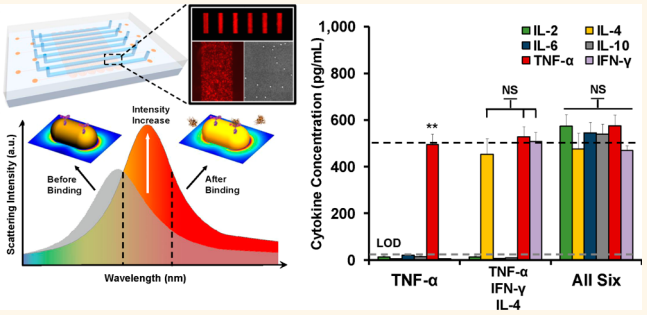

KEYWORDS: localized surface plasmon resonance (LSPR) · nanoplasmonic sensing · optofluidics · multiplexed immunoassay · serum cytokines

Cytokines are bioactive proteins responsible for dynamic regulation of the maturation, growth, and responsiveness of immune cells.[1,2] Quantifying cytokines in human serum provides highly valuable clinical information to monitor the immune status of hosts and adjust therapies in different inflammatory disease conditions, such as sepsis,[3] cancer,[4] lupus,[5] and graft-*versus*-host disease (GVHD).[6] Given the complexity and dynamic nature of the human immune system, detection and trending of biomarker signatures and their subtle changes occurring during a diseased state requires rapid analysis of a complex panel of multiple cytokines at high accuracy, sensitivity and throughput. However, conventional methods based on sandwich immunoassays fall short of meeting this demand as they present stringent limitations on their practical implementation as immune monitoring approaches. These limitations arise primarily from their needs for multiple time-consuming labeling and washing processes while consuming a large sample volume. At present, no assay exists

* Address correspondence to katsuo@umich.edu.

Received for review January 19, 2015 and accepted March 19, 2015.

Published online March 20, 2015
10.1021/acsnano.5b00396

that satisfies all the requirements of near-real-time immune status monitoring that involve analysis of complex biological samples (such as human blood) in miniature quantities.

Over the last two decades, plasmonic biosensing has drawn much attention as a potential alternative to fluorescence-based methods that enables fast, real-time label-free detection of biological species.[7−9] Plasmonic biosensing has demonstrated rapid sensing response, limited reaction to external interferences, high stability in harsh environments, and noninvasiveness to test samples. Driven by modern advances in nanofabrication, plasmonic biosensing technologies have evolved into nanobiosensing based on localized surface plasmon resonance (LSPR),[10−13] where surface binding of analyte molecules is detected in real time from a shift in photon absorbing and scattering behaviors of collectively oscillating conduction-band electrons highly localized on the surfaces of metallic nanoparticles.[11] With emerging nanoplasmonic biosensing technologies and microdevice fabrication techniques, integration of miniaturized LSPR biosensors into highly functional microfluidic chips with liquid sample handling capability is a promising approach toward practical biomarker screening.[14−16] However, the implementation of such sensors for protein biomarker detection in complex clinically relevant samples is still in infancy. Furthermore, nanoplasmonic biosensing in clinical and pharmaceutical settings has been prohibited by the inability to simultaneously achieve high sensitivity and assay speed.

Here we have developed a highly practical, multiarrayed LSPR chip for massively parallel high-throughput detection of multiple cytokine biomarkers in miniature quantities of serum samples. The LSPR microarray device was fabricated using easy-to-implement, one-step microfluidic patterning and antibody conjugation of gold nanorods (AuNRs). Scanning the scattering light intensity across the microarrays of AuNR ensembles with dark-field imaging optics, our biosensing technique allowed for quantitative cytokine measurements at concentrations ranging from 10 to 10 000 pg/mL in a 1 μL sample of serum. In only 40 min we completed the whole parallel on-chip assays, which involved the manual loading, incubation, and washing of 8 different samples, and multianalyte detection repeated 10 times for each sample using the entire 480 LSPR biosensor arrays. In contrast, conventional sandwich immunoassays take more than 10 times as long to complete. The microarray biochip assay only required simple manual sample/reagent pipetting processes and a readily available standard optical microscopy setup. With the validation of the LSPR microarray assay with an enzyme-linked immunosorbent assay (ELISA) and successful demonstration of its functionality with clinical samples, our study has taken the first significant step toward translating nanoplasmonic biosensing technology to its practical use in serum cytokine-based immune status monitoring.

RESULTS AND DISCUSSION

LSPR Microarray Chip Preparation. Our LSPR microarray biochip consists of eight parallel microfluidic channels which run orthogonal to six meandering stripes of antibody-functionalized AuNR ensembles (characteristic properties of the AuNRs are shown in Supporting Information Figure S1) with 10 turns on a glass substrate (Figure 1a). Each microfluidic channel can hold 250 nL in volume and has inlet and outlet ports for reagent loading and washing. This chip design gives rise to an array of 480 stripe-shaped LSPR biosensing spots (25 μm × 200 μm) on the entire chip. Here, using a one-step microfluidic patterning technique (Supporting Information Figure S2), we conjugated the AuNR stripes with antibodies against six different cytokines: interleukin-2 (IL-2), interleukin-4 (IL-4), interleukin-6 (IL-6), interleukin-10 (IL-10), interferon-gamma (IFN-γ), and tumor-necrosis-factor alpha (TNF-α). Microfluidic flow-patterning technique has been successfully demonstrated to create patterns of antibodies/biomolecules on glass substrates and gold thin film in previous studies.[17,18] However, this approach has not yet been employed to fabricate LSPR based biosensor spots with flexible geometry that can be readily manipulated. The six cytokines employed in this study are known to yield predictive values indicating the development of organ damage and bacterial infections.[19,20] The microfluidic patterning technique allowed us to construct 10 segments of six collocating parallel multiplex immunoassay spots in each channel without cumbersome manual reagent dispensation on the large number of locations (Figure 1a). We utilized scanning electron microscopy to validate that the LSPR sensing spots were coated with a disordered monolayer of AuNR particles at a surface number density of ~1 particles per 2.56 μm^2 (Figure 1a and Supporting Information Figure S3), which corresponded to an average particle-to-particle distance greater than 200 nm (Figure 1b). Our theoretical calculation predicted a much shorter (65 nm) decay length of the highly localized photoexcited EM field surrounding each nanoparticle (Inserted panel of Figure 1b). Thus, the dispersed distribution of AuNRs effectively eliminated electromagnetic couplings between neighboring nanoparticles in the LSPR biosensing ensembles. As a result, the multiarrayed LSPR sensor performance was solely determined by the superimposition of the optical characteristics of individual nanoparticles while uninfluenced by the disordered nanoparticle arrangement. Therefore, the ensemble of ~2000 plasmonically uncoupled AuNRs on each sensor spot could yield a scattering spectrum with a distinct resonance without particle-to-particle electromagnetic interferences (Figure 1c). Variance in this resonance could be

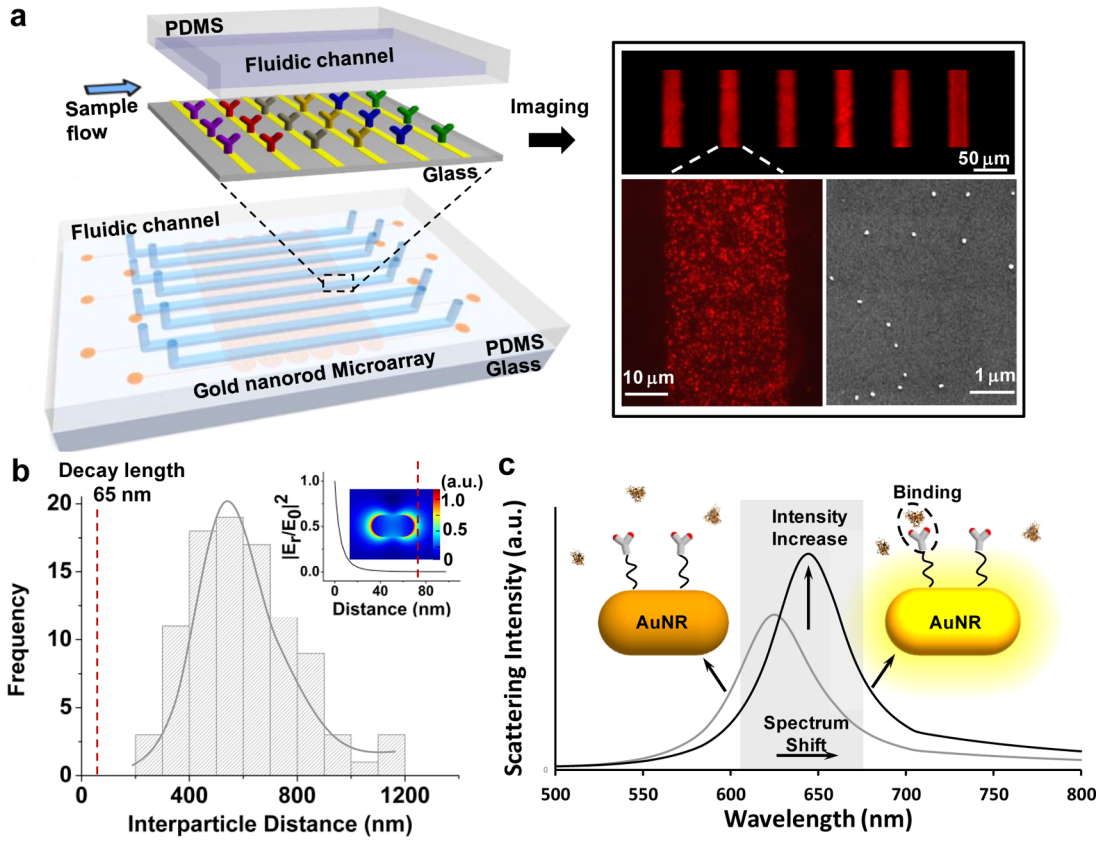

Figure 1. Schematic and principle of the method. (a) Schematic of the LSPR microarray chip. The nanorod microarray fabrication was performed using a one-step microfluidic patterning technique assisted by electrostatic attractive interactions between the nanorods and the substrate surface within microfluidic channels (Materials and Methods and Supporting Information Section 2). Subsequently, these nanorode microarrays were integrated in a microfluidic chip with eight parallel microfluidic detection channels consisting of inlet and outlet ports for reagent loading and washing. Specific antibodies were conjugated to the patterned AuNR microarrays using thiolated cross-linker and EDC/NHC chemistry. The current chip design integrates 480 AuNR microarray sensor spots. The prepared LSPR microarray chip was then imaged under dark-field microscopy and scanning electron microscopy (SEM). (b) Histograms of the particle-to-particle distance of the AuNRs on the LSPR microarray chip characterized using SEM images. The resulted interparticle distance was measured to be >200 nm, much larger than the decay length of the localized electric field on the AuNR surface as shown in the inserted EM simulation. (c) The principle of the LSPR microarray method. Analyte molecules are introduced to an antibody-functionalized AuNR LSPR biosensor. Binding of the analyte molecules to the receptors induces a redshift and scattering intensity change of the longitudinal SPR (exaggerated in the illustration). This intensity change is imaged *via* the characteristic frequency (gray area) using EMCCD coupled dark-field microscopy.

effectively exploited for detecting target analyte binding onto the AuNR.

Dark-Field Imaging and Material Selection. Despite the impressive rapidness, sample efficiency, and throughput, multiarrayed LSPR biochip schemes for serum cytokine screening would face a major issue - poor limit of detection (LOD). For instance, major efforts have been made to identify serum cytokine profiles useful for either the early detection of sepsis or to assess illness severity.[21,22] Serum cytokine concentrations for patients with sepsis can vary widely necessitating both a wide dynamic range and low LOD to provide meaningful information with clinical utility. Bozza *et al.* reported the ability to predict 28-day mortality in patients with sepsis by measuring serum IL-8 within the first 72 h of admission.[22] A serum IL-8 cutoff able to meaningfully discriminate between survivors and nonsurvivors with reasonable accuracy would be an assay capable of measuring serum cytokines concentrations less than 100 pg/mL. This cutoff value is already comparable to or far below the LOD's obtained by previous studies.[14,23] To achieve such high sensitivity, our detection method employed dark-field imaging that scans the scattering light intensity across the LSPR biosensing spots (Supporting Information Figure S4). In the extreme case, LSPR biosensing technology can even detect single-molecule binding events using a single nanoparticle.[24,25] However, the use of an isolated nanoparticle-biosensor becomes impractical in clinical settings since it requires either highly challenging handling of extremely small volume samples or sample dilution that results in an impractical, time-consuming assay governed by very slow analyte binding kinetics.[26] Instead, probing the optical signature of the nanoparticle ensembles provides significant advantages for practical sensor development.[27,28]

Analyzing the optical signal from these ensembles inherently contains statistically and biologically meaningful information across a large number of nanoparticle biosensors. Such information can be obtained with high tolerance against variances and irregularities of individual nanoparticle structures and spatial arrangement as those observed with our LSPR microarray chip (Figure 1a). Our theoretical model in the Supporting Information Sections 5 and 6 predicts that this approach would result in a LOD value more than ten times lower than that of spectrum-shift detection schemes commonly used in conventional label-free LSPR biosensing. The rod shape and size (40 nm in width, aspect ratio (width/height): 2) of our sensor nanoparticles were specifically selected to yield optimal sensing performance[29] with small LOD values. The nanoparticles were engineered to yield high sensitivity to the local refractive index and display a distinct intensity change resulting from a redshift in the resonant Rayleigh scattering spectrum upon analyte surface binding.[11,30,31] Additionally, we anticipate a large detection dynamic range for the nanoparticle ensemble analysis scheme, which provides a large number of binding sites for a given number of analyte molecules in a sample.

Real-Time LSPR Multiplex Immunoassay. Characterizing the dynamic performance of LSPR biosensors allows us to assess the total assay time. To this end, we measured real-time sensor signal variations associated with analyte surface binding in a multiplex scheme with a mixture of the six target cytokines suspended in phosphate buffered saline (PBS) solution. In the cytokine solution, a different concentration level was assigned to each analyte such that IL-2, IL-4, IL-6, IL-10, TNF-α, and IFN-γ were at 10 000, 5000, 3000, 1000, 500, and 250 pg/mL, respectively. We loaded the cytokine mixture into one of the microfluidic channels of the LSPR microarray device and subsequently observed the time-course signal variation from the sensor spots (Figure 2). Analyte-binding events reached an equilibrium within 30 min after the introduction of the cytokine mixture into the LSPR microarray device, as evidenced by signal plateaus. The rapid analyte binding kinetics allowed the assay to be performed with a very short incubation time as compared to conventional sandwich immunoassays. After the analyte-binding equilibrium was reached, the loaded samples were flushed with PBS to remove nonspecifically bound serum constituents from the sensor surfaces. This resulted in a sensor signal intensity reduction by ~8% on average across the six concentration conditions.

Relying upon the measurement of labeling signals, conventional sandwich immunoassays often employed in ELISA (*e.g.*, DuoSet ELISA, R&D system) provide the end-point analyte readout only after the completion of all the multiple reagent processes. Without the end-point time being precisely known, users of these assay techniques need to follow a protocol requiring 2 h only for the analyte incubation. Additional labeling and washing steps together with the time-consuming incubation process result in a typical total assay time of 8 h or longer. In contrast, both the label-free nature and real-time analyte binding monitoring capability demonstrated in this study are highly notable features of the LSPR microarray immunoassay. These features allowed us to eliminate the multistep assay processes and reduce the analyte incubation time to less than 30 min as described above. From the real-time sensor signal saturation point, we were able to determine the end-point of the analyte-binding assay where we could immediately initiate the washing process to remove the nonspecifically adsorbed analyte molecules. This allowed the entire LSPR microarray immunoassay involving the parallel sample loading, multianalyte (IL-2, IL-4, IL-6, IL-10, TNF-α, and IFN-γ) binding, incubation, and washing across the 480 on-chip biosensing spots to be completed within a short period of time.

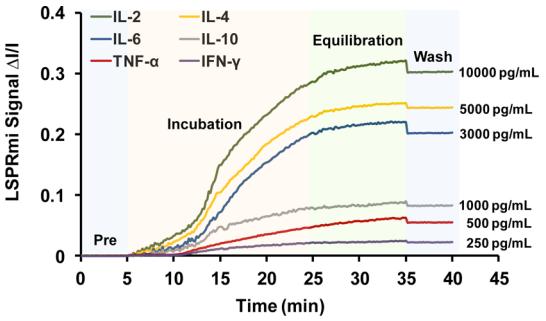

Figure 2. Real-time AuNR microarray signals during the multiplex cytokine detection. The blue region shows the LSPR microarray signal during the preloading. The orange and green regions show the transient increase and final equilibration of LSPR microarray signals, respectively, during incubation following the sample loading. The gray region shows the LSPR microarray signal after washing.

High-Throughput LSPR Microarray Biosensing and Calibration. A significant feature of our LSPR microarray chip assay is its ability to analyze the multiple analytes simultaneously at high throughput. We demonstrated this capability by performing massively parallel data-intensive sensor calibration using the LSPR microarray device within a short period of time. Calibration data obtained for each analyte subsequently allowed us to determine the dynamic range and detection limit of our assay for each target analyte. To this end, we prepared eight PBS samples, each spiked with a mixture of the six purified cytokine species (IL-2, IL-4, IL-6, IL-10, IFN-γ, and TNF-α), and manually pipetted the samples into the inlets of the eight channels of the device (Figure 3a). For one channel, all of the cytokines had the same concentration, one of the values 50 to 10 000 pg/mL. The sensor response was recorded over 480 individual AuNR microarray sensing spots on the same chip at a scanning rate of 180 spots/min.

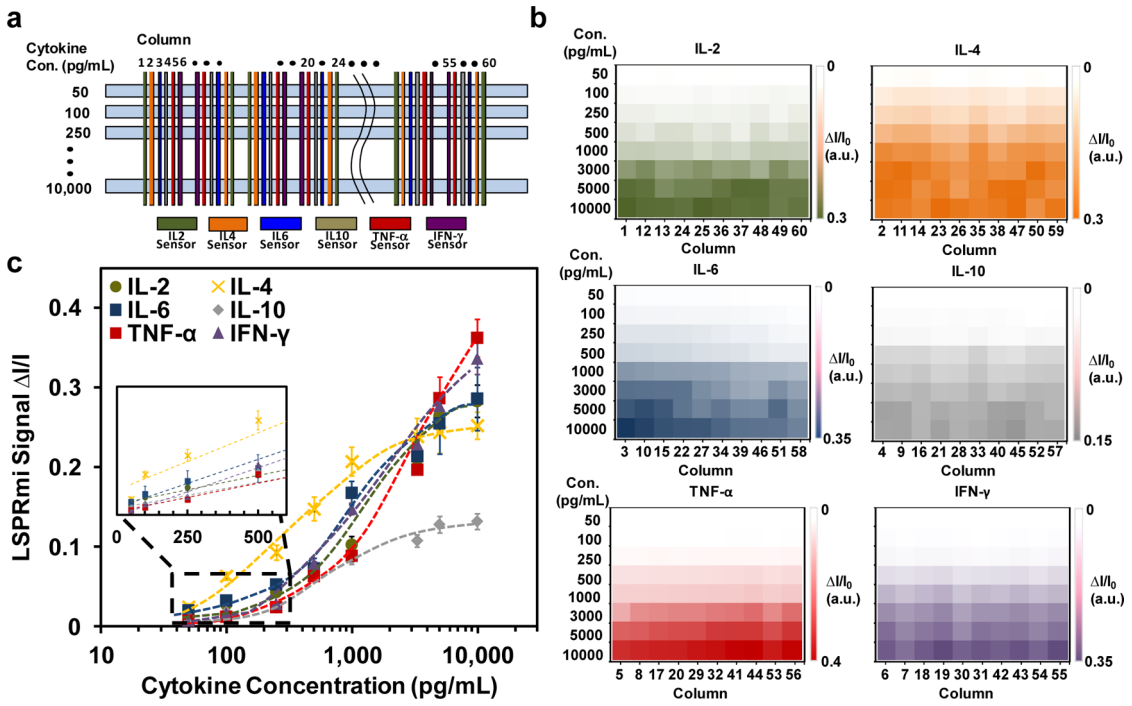

Figure 3. LSPR microarray intensity mapping and calibration curves obtained by a massively parallel on-chip assay. (a) LSPR microarray chip layout consisting of 60 antibody-functionalized AuNR stripes segmented by 8 microfluidic detection channels. This layout results in 480 total sensor spots on a single chip. The target cytokine at each AuNR stripe is color-coded. The sensor calibration was performed for the 480 sensor spots in a massively parallel manner by sequentially loading purified solutions of IL-2, IL-4, IL-6, IL-10, TNF-α, and IFN-γ into each detection channel and detecting the LSPR signals of the multiple sensor spots. The cytokine concentrations introduced to the detection channels are 50 pg/mL in Channel 1; 100 pg/mL in Channel 2; 250 pg/mL in Channel 3; 500 pg/mL in Channel 4; 1000 pg/mL in Channel 5; 3000 pg/mL in Channel 6; 5000 pg/mL in Channel 7; and 10 000 pg/mL in Channel 8. These concentration values are set to be the same for all the six cytokines in each channel. (b) Mapping of LSPR signal intensity shifts over the 480 AuNR barcode sensor spots on the LSPR microarray chip obtained by the multianalyte calibration process for the six cytokines in (a). The process enables the 480-spot signal reading within 5 min after loading, incubating, and washing these cytokines. The intensity unit is arbitrary unit obtained from the EMCCD. (c) Calibration curves of TNF-α, IFN-γ, IL-2, IL-4, IL-6, IL-10 obtained from the LSPR barcode intensity mapping in (b). The dashed lines represent the sigmoidal curves fitted to data points. The inserted figure shows the linear region of the calibrations curves at low concentrations.

Thus, the total assay time including sample loading and washing (5 min), incubation and equilibration (30 min), and image scanning (5 min) was around 40 min. Figure 3b shows a result of mapping the local intensity variation ($\Delta I/I_0$) after loading and washing cytokine molecules over 480 sensor spots, where I_0 is the original sensor signal intensity prior to the assay and ΔI is the intensity shift after the assay. We then obtained sensor calibration curves for the six cytokines by plotting the normalized intensity shift $\Delta I/I_0$ spatially averaged over 10 sensor spots as a function of analyte concentration (Figure 3c). We further verified that these measurements were consistent across ten sensor spot replicates with an averaged coefficient of variance around 7% as described in the Supporting Information Section 7. The calibration curves confirm that the assay could achieve a large dynamic range from 10 to 10 000 pg/mL for each of the six cytokine biomarkers. The dashed lines in the plots represent sigmoidal curves fitted to data points (Hill type). We determined the LOD for each analyte as defined by $3\sigma/k_{slope}$, where σ and k_{slope} are the standard deviation of background signal obtained from a blank control and the regression slope of each calibration curve, respectively. The determined LOD's for the six cytokines were 11.43 (TNF-α), 6.46 (IFN-γ), 20.56 (IL-2), 4.60 (IL-4), 11.29 (IL-6), and 10.97 pg/mL (IL-10) as summarized in Supporting Information Table S1. Notably, the LOD's and dynamic range of the LSPR microarray assay are comparable to the gold standard, singleplex ELISA, and surpass most of the existing multiplex ELISA assays.[32]

Multiplex LSPR Microarray Immunoassay of Serum Cytokines. To validate the multiplex immunoassay capability of the LSPR microarray, we prepared a set of serum samples using heat inactivated and charcoal absorbed human serum and spiked them with different mixtures of the six cytokines. Using these spiked samples, we obtained postassay signal images for the panel of the six striped sensing spots integrated within the same microfluidic channel, where a sample of particular cytokine mixture pattern was loaded. We observed that the signal intensity of each sensor array was dependent on the target cytokine and independent of the presence of off-target cytokines in the serum solution (Figure 4a). The intensity shift measured from

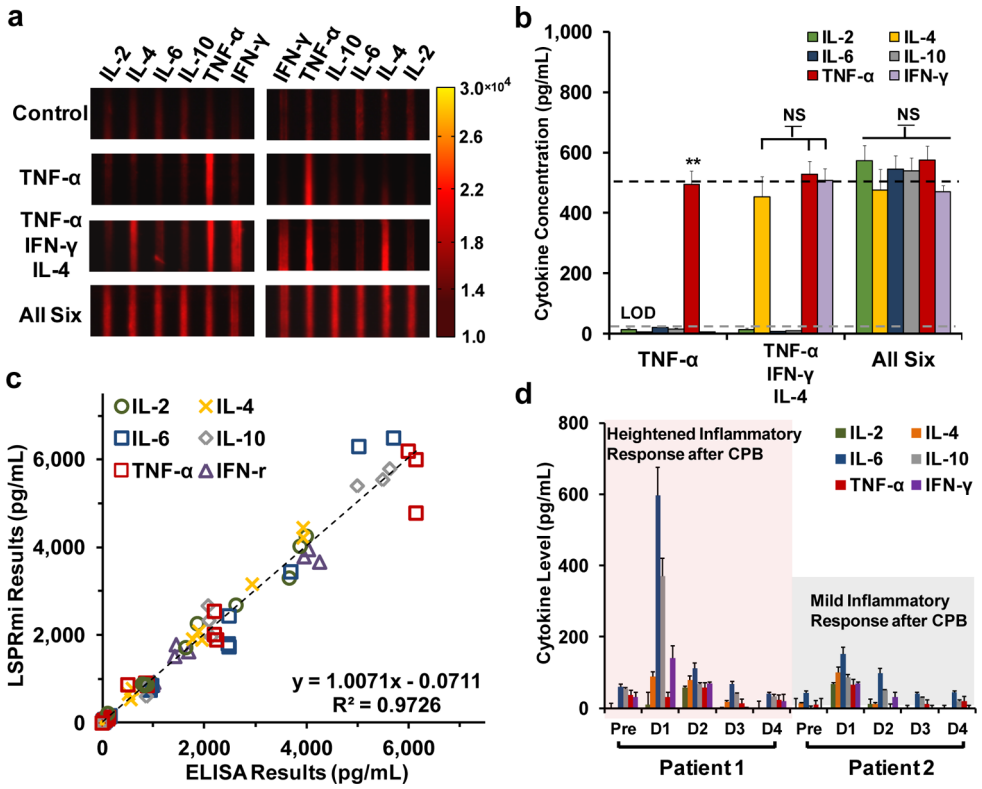

Figure 4. Multiplex cytokine detection in healthy donor serum matrix and patient serum samples. (a) Dark-field images of AuNR microarrays within a single microfluidic detection channel loaded with different sample mixtures of recombinant cytokines spiked in serum matrix. The concentration of every cytokine in the mixtures is 500 pg/mL. (b) Cytokine concentrations quantified for the samples in (a). Measuring the scattering light intensities of the barcodes and converting them to concentration values using calibration curves allowed for the quantification of the cytokine concentrations. The dashed line in black represents the predetermined value (500 pg/mL) of the analyte concentration. The dashed line in gray represents the limit of detection (LOD) of the LSPR microarray mesurement. (c) Correlation between data obtained from the LSPR microarray assay and gold standard ELISA for the spiked-in serum samples with cytokine concentrations ranging from 32 to 5000 pg/mL. (d) Five-day cytokine concentration variations measured by the LSPR microarray assay for serum samples extracted from two post-CPB-surgery pediatric patients. The patients were discharged from the pediatric intensive care unit (PICU) after the five-day blood sampling since clinicians determined that their health conditions returned to normal then. Statistical analysis of experimental data with respect to both the recombinant protein and stimulated PBMCs controls: *, *p*-value < 0.05; **, *p*-value < 0.01; NS, no significant difference (Student *t* test).

the LSPR microarray was translated into analyte concentration using the calibration curves in Figure 4b. We found no statistically significant difference between the measured cytokine concentrations and their expected values of 500 pg/mL. Furthermore, the sensors targeting cytokines absent from the serum matrix yielded signals below their LOD as anticipated. We also calculated the percent recovery, which is defined to be the amount of analyte detected as the fraction of the amount of known analyte in a sample. The percent recovery for all cytokines fell within an acceptable range of 85−115% (data not shown).[33] Thus, our multiplex assay exhibited minimum cross-reactivity among the six cytokines biosensors.

Nonspecific antibody cross-reactions pose significant challenges in retaining high accuracy for multiplex sandwich immunoassays. This issue becomes serious when the assay involves a large number of antibody pairs in a complex biological medium, such as human serum. It prevents the scaling up of multiplexing because nonspecific bindings among antibodies, target analytes and other biological components in the solution (*e.g.*, free plasma proteins, lipids, electrolytes, *etc.*) exponentially increase. Since the LSPR biosensing scheme is label-free, it is free from the complications of the secondary antibody labeling. The direct measurement of the sensor response upon analyte binding substantially quenched the nonspecific adsorption among all the biological species. As a result, our assay displayed the negligible cross-reactivity.

Assay Validation with the Gold Standard Method. Wide acceptance of a new multiplex immunoassay method requires its full validation with the existing "gold-standard" assay: ELISA. Here, we prepared healthy-donor serum samples spiked with a mixture of the six cytokines at concentrations ranging across the entire dynamic range of our assay and performed multiplex immunoassay using our LSPR microarray chip. Together with our assay, we performed ELISA-based measurements for the same samples. The ELISA-based measurements were based on the singleplex scheme. In other words, the assay targeted only one of the six

cytokines in each measurement to avoid any potential crosstalk between different probe molecules. We repeated the singleplex ELISA measurements for all the six cytokines across the serum samples prepared above. Finally, we compared our LSPR microarray immunoassay measurements with the ELISA measurements and observed an excellent linear correlation ($R^2 = 0.9726$) between results generated from the both methods (Figure 4c). The LSPR microarray assay showed a significantly better correlation with singleplex ELISA than the commercial multiplex bead array assays (MBAA) for human serum analysis.[22] Correlations coefficients between MBAA and ELISA, reported in both peer reviewed studies as well as the product literature from commercial vendors, vary widely and can be as low as 0.75, resulting in high degrees of uncertainty when depending on these assays for clinical decision making.[22] It is worth noting that the size and number of the AuNR microarrays in our assay can be readily tuned by changing the microfluidic patterning conditions. This suggests that our multiplex immunoassay exhibits great potential for even higher multiplexing without being limited by antibody cross-reactions that are generally associated with conventional multiplex immunoassays.

Immune Status Monitoring of Infant Patients with Cardiopulmonary Bypass Surgery. Leveraging the strengths of our LSPR microarray immunoassay, we sought to demonstrate the utility of our technology to allow monitoring of the inflammatory response of neonates following cardiothoracic surgery necessitating cardiopulmonary bypass (CPB). Repair of congenital heart defects, the most common birth defect in the United States,[34] necessitates open heart surgery using CPB to supplant heart−lung function during surgery. Blood contact with the artificial surfaces of the CPB circuit is known to elicit a substantial inflammatory response in the immediate postoperative period that is normally restored to preoperative levels within 48 h after surgery.[35] As a proof-of-concept, we collected serum samples prior to surgery (Pre) and on postoperative days one (D1), two (D2), three (D3), and four (D4) from two neonates undergoing congenital heart surgery with CPB and used our LSPR microarray immunoassay to quantify circulating serum cytokine levels in these samples (Figure 4d). We observed increased levels of both IL-6 and IL-10 on D1 following CPB in both patients although they were expressed at different levels. Postoperative heightening was also observed for IL-2, IL-4, TNF-α, and IFN-γ in these patients on D1 or D2. The elevated cytokine expression was followed by a return to preoperative levels of all the measured cytokines on D3 and D4. We observed a very similar pattern to those previously reported where elevations in patient's serum cytokine levels most commonly return to presurgical levels within 48 h of surgery. Such information has proven valuable since it is known that very high and/or prolonged expression of both pro-inflammatory (*e.g.*, IL-6) and anti-inflammatory (*e.g.*, IL-10) cytokines is associated with the acute immune dysfunction following cardiopulmonary bypass and can predict worse outcomes.[36,37] This pattern of expression is thought to result from the host's misregulated compensatory effort to counter an initial pro-inflammatory response that occurs perioperatively as a result of cardiopulmonary bypass.[36,37] Most importantly, the LSPR microarray assay was capable of detecting variable degrees of responses in the two subjects after CPB. There are multiple mechanisms contributing to this variable cytokine expression (*e.g.*, patient age, cardiac lesion, length of surgery and CPB, use of intraoperative steroids, *etc.*); however, no methodology exists to safely, routinely, and repetitively measure serum cytokines in near real-time to enable clinicians to monitor a host inflammatory response and thereby potentially alter therapeutic strategies.

CONCLUSION

In conclusion, we have developed a label-free LSPR microarray immunoassay that enables the high-throughput analysis of multiple immune biomarkers in a rapid, accurate, easy-to-implement, and sensitive manner. Over the past years, researchers have used LSPR-based biomolecular binding assays as an emerging label-free optical biosensing technique enabled by recent advances in nanotechnology. We have further advanced the assay technology to the extent that it becomes ready for its translation to clinical use. The key to our successful outcome is attributed to synergistically employing microfluidics-enabled patterning and dark-field imaging of AuNR LSPR microarray biosensors.

To our best knowledge, our study is the first to demonstrate the LSPR-based time-course multiplex serum cytokine detection under the clinical scenario where the powerful features of our assay technology are most pronounced. The LSPR microarray assay successfully measured elevated cytokine levels, most notably for IL-6 and IL-10, in two neonates at 24 h after cardiopulmonary bypass surgery for congenital heart disease. Obtaining the serum samples from CPB-surgery pediatric patients, we could exactly define the source of the inflammatory response of the hosts—the surgery,—and predicted the anticipated assay outcomes. The cytokine expression profile measurements demonstrated here have proved our capability to routinely monitor multiple serum cytokines in critically ill neonates using the LSPR microarray assay. The rapid turn-around time (~40 min), high sensitivity (down to ~6.46−20.56 pg/mL), extreme sample sparing ability (~1 μL sample for six cytokines with 10 technical replicate measurements) and negligible cross-reactivity enable routine monitoring of serum cytokines with statistically high accuracy. Such characteristics position

this LSPR microarray platform to have relevant application in a substantial number of different disease states—particularly in infants and neonates where sample volume has been a militating actor. Such key characteristics do not exist with current methods as the assay turn-around time and blood volume required make them impractical to use, especially in small infants.

The multiplex immunoassay using our biosensing platform can generally serve as a powerful tool for the detection of a wide spectrum of biomarkers relevant to human disease screening and drug discovery. A clinical study to validate a pediatric sepsis biomarker risk model using an extended version of our current technology is underway at the University of Michigan C.S. Mott Children's Hospital. Our platform can also extend into the basic science arena providing small volume rapid detection of proteins from cell media or animal serum with excellent correlation to standard ELISA detection methods. Theoretically, our LSPR sensor spot size can be scaled down to $\sim$100 μm^2 assuming that each microarray requires a minimum number of AuNRs to maintain its statistical accuracy (= 40). Such a small sensor spot would make it possible to integrate our LSPR microarray sensors in functional micro- and nanofluidic systems to enable multiplex cytokine secretion assay with single cells.

MATERIALS AND METHODS

LSPR Microarray Chip Fabrication. Positively charged AuNRs (CTAB coating) used in this study were purchased from Nanoseedz. The AuNRs were patterned on an oxygen plasma treated glass substrate using a microfluidic patterning technique through electrostatic interactions between the AuNRs and the glass surface. The constructed AuNR barcode patterns were functionalized with thiolated alkane 10-carboxy-1-decanethiol ($HS-(CH_2)_{10}-COOH$) through ligand exchange and subsequently activated using standard EDC/NHS coupling chemistry. The probe cytokine antibodies were then loaded into individual patterning channels, forming a barcode array consisting of six parallel stripes each functioned with distinct antibodies to afford multiplex detection of 6 different cytokines at one time (details in Supporting Information Sections 2 and 3).

LSPR Microarray Assay Protocol. The prepared LSPR microarray assay chip was mounted on a motorized stage (ProScanIII, Prior Scientific, Rockland, MA) that allowed for 3D positioning and automated image scanning. The back of the glass substrate of the chip was attached with a dark-field condenser (NA = 1.45, Nikon) *via* the lens oil. Then, 250 nL of sample was injected from the inlet, flown through the sample channel, and collected from the outlet. The light scattered from the sensor microarrays was collected by the 10× objective lens beneath the assay chip, filtered by a band-pass filter (610−680 nm), imaged by an electron-multiplying CCD (EMCCD, Photometrics, Tucson, AZ) camera and recorded using the NIS-Element BR analysis software. The obtained images were then analyzed by a customized Matlab program. Before each measurement, we waited for $\sim$10 min to establish temperature stabilization of the EMCCD to minimize the background signal drift (details in Supporting Information Section 4).

LSPR Microarray Assay Human Serum Matrix Multiplex Performance Characterization. To characterize both the multiplex capability and our assay's performance, we created three separate mixtures of cytokines. One mixture contained a single cytokine species (TNF-α), another containing three cytokines (IL-4, IFN-γ, and TNF-α), and finally one containing all six cytokines (IL-2, IL-4, IL-6, IL-10, IFN-γ, and TNF-α). Recombinant cytokines (Life Technologies, Frederick, MD) were spiked into a commercially available heat-inactivated, charcoal absorbed human serum matrix to remove trace levels of cytokines (EMD Millipore, St. Charles, MO).

LSPR Microarray Assay Performance Comparison to "Gold Standard" ELISA. All six cytokines (IL-2, IL-4, IL-6, IL-10, IFN-γ, TNF-α) were spiked into healthy donor human serum obtained *via* venipuncture following informed written consent. The study was approved by the University of Michigan Institutional Review Board. Serum was obtained *via* venipuncture into vacutainer tubes containing clot activator (BD Diagnostics, Franklin Lake, NJ). Tubes were processed according to the manufacturer's instructions. Serum samples doped with all six cytokines were diluted further with healthy donor serum to obtain samples across the entire dynamic range of our LSPR microarray assay (32 −5000 pg/mL). Serum cytokine concentrations were quantified using our LSPR microarray assay and compared to commercially available ELISA kits (IL-6, IL-10, IFN-γ, TNF-α, BioSource Europe S.A., Nivelles, Belgium; IL-2, IL-4, Thermo-Fisher Scientific, Rockford, IL).

LSPR Microarray Assay for Serum Cytokine Quantification of Neonatal Patients Follwoing Open-Heart Surgery with Cardiopulmonary Bypass. All studies described here were approved by the University of Michigan Institutional Review Board and conducted following informed parental consent. Briefly, we randomly chose two patients enrolled in an ongoing clinical trial for serum cytokine quantification. Serum samples were collected prior to surgery and then on postoperative days one, two, three, and four (Pre, D1, D2, D3, and D4, respectively) using a SST microtainer (BD Diagnostics) according to the manufacturer's instructions. Serum cytokines (IL-2, IL-4, IL-6, IL-10, IFN-γ, TNF-α) were quantified using our LSPR microarray immunoassay as described above.

FDTD Simulations. The limit of detection of the LSPR microarray measurement was theoretically estimated by performing a finite difference time domain (FDTD) simulation that predicted the scattering efficiency on a AuNR. The simulation used commercial multiphysics simulation software, COMSOL (details in Supporting Information Section 5).

Conflict of Interest: The authors declare no competing financial interest.

Acknowledgment. This work was supported by the National Institute of Health (Grant No. R01 HL119542-01A1) and National Science Foundation (Grant No. CBET 1263889). R.N. thanks for the Michigan Institute for Clinical & Health Research for support under the Postdoctoral Translational Scholars Program by Grant Number 2UL1TR000433 from the National Center for Advancing Translational Sciences. The content is solely the responsibility of the authors and does not necessarily represent the official views of NCATS or the National Institutes of Health.

Supporting Information Available: Additional information is noted in the text. This material is available free of charge *via* the Internet at http://pubs.acs.org.

REFERENCES AND NOTES

1. Opal, S. M.; DePalo, V. A. Anti-Inflammatory Cytokines. *Chest* **2000**, *117*, 1162–1172.
2. Rothenberg, E. V. Cell Lineage Regulators in B and T Cell Development. *Nat. Immunol.* **2007**, *8*, 441–444.
3. Damas, P.; Canivet, J. L.; de Groote, D.; Vrindts, Y.; Albert, A.; Franchimont, P.; Lamy, M. Sepsis and Serum Cytokine Concentrations. *Crit. Care Med.* **1997**, *25*, 405–412.
4. Lippitz, B. E. Cytokine Patterns in Patients with Cancer: A Systematic Review. *Lancet Oncol.* **2013**, *14*, E218–E228.
5. Maczynska, I.; Millo, B.; Ratajczak-Stefanska, V.; Maleszka, R.; Szych, Z.; Kurpisz, M.; Giedrys-Kalemba, S. Proinflammatory

Cytokine (IL-1 beta, IL-6, IL-12, IL-18 and TNF-alpha) Levels in Sera of Patients with Subacute Cutaneous Lupus Erythematosus (SCLE). *Immunol. Lett.* **2006**, *102*, 79–82.
6. Visentainer, J. E. L.; Lieber, S. R.; Persoli, L. B.; Vigorito, A. C.; Aranha, F. J.; de Brito Eid, K. A.; Oliveria, G. B.; Miranda, E. C.; de Souza, C. A. Serum Cytokine Levels and Acute Graft-*versus*-Host Disease after HLA-Identical Hematopoietic Stem Cell Transplantation. *Exp. Hematol.* **2003**, *31*, 1044–1050.
7. Homola, J. Surface Plasmon Resonance Sensors for Detection of Chemical and Biological Species. *Chem. Rev.* **2008**, *108*, 462–493.
8. Mariani, S.; Minunni, M. Surface Plasmon Resonance Applications in Clinical Analysis. *Anal. Bioanal. Chem.* **2014**, *406*, 2303–2323.
9. Sipova, H.; Homola, J. Surface Plasmon Resonance Sensing of Nucleic Acids: A Review. *Anal. Chim. Acta* **2013**, *773*, 9–23.
10. Mayer, K. M.; Hafner, J. H. Localized Surface Plasmon Resonance Sensors. *Chem. Rev.* **2011**, *111*, 3828–3857.
11. Anker, J. N.; Hall, W. P.; Lyandres, O.; Shah, N. C.; Zhao, J.; Van Duyne, R. P. Biosensing with Plasmonic Nanosensors. *Nat. Mater.* **2008**, *7*, 442–453.
12. Jones, M. R.; Osberg, K. D.; Macfarlane, R. J.; Langille, M. R.; Mirkin, C. A. Templated Techniques for the Synthesis and Assembly of Plasmonic Nanostructures. *Chem. Rev.* **2011**, *111*, 3736–3827.
13. Kabashin, A. V.; Evans, P.; Pastkovsky, S.; Hendren, W.; Wurtz, G. A.; Atkinson, R.; Pollard, R.; Podolskiy, V. A.; Zayats, A. V. Plasmonic Nanorod Metamaterials for Biosensing. *Nat. Mater.* **2009**, *8*, 867–871.
14. Acimovic, S. S.; Ortega, M. A.; Sanz, V.; Berthelot, J.; Garcia-Cordero, J. L.; Renger, J.; Maerkl, S. J.; Kreuzer, M. P.; Quidant, R. LSPR Chip for Parallel, Rapid, and Sensitive Detection of Cancer Markers in Serum. *Nano Lett.* **2014**, *14*, 2636–2641.
15. Oh, B. R.; Huang, N. T.; Chen, W.; Seo, J.; Chen, P.; Cornell, T. T.; Shanley, T. P.; Fu, J.; Kurabayashi, K. Integrated Nanoplasmonic Sensing for Cellular Functional Immunoanalysis Using Human Blood. *ACS Nano* **2014**, *8*, 2667–2676.
16. Brolo, A. G. Plasmonics for Future Biosensors. *Nat. Photonics* **2012**, *6*, 709–713.
17. Bronner, V.; Bravman, T.; Nimri, S.; Lavie, K. Rapid and Efficient Determination of Kinetic Rate Constants Using the ProteOn XPR36 Protein Interaction Array System. *Bio-Rad Bull.* **2006**, 3172.
18. Ma, C.; Fan, R.; Ahmad, H.; Shi, Q.; Comin-Anduix, B.; Chodon, T.; Koya, R. C.; Liu, C. C.; Kwong, G. A.; Radu, C. G.; et al. A Clinical Microchip for Evaluation of Single Immune Cells Reveals High Functional Heterogeneity in Phenotypically Similar T Cells. *Nat. Med.* **2011**, *17*, 738–744.
19. Wang, J. Y.; Wang, X. L.; Liu, P. Detection of Serum TNF-alpha, IFN-gamma, IL-6 and IL-8 in Patients with Hepatitis B. *World J. Gastroenterol.* **1999**, *5*, 38–40.
20. Ray, C. A.; Bowsher, R. R.; Smith, W. C.; Devanarayan, V.; Willey, M. B.; Brandt, J. T.; Dean, R. A. Development, Validation, and Implementation of a Multiplex Immunoassay for the Simultaneous Determination of Five Cytokines in Human Serum. *J. Pharm. Biomed. Anal.* **2005**, *36*, 1037–1044.
21. Wong, H. R.; Salisbury, S.; Xiao, Q.; Cvijanovich, N. Z.; Hall, M.; Allen, G. L.; Thomas, N. J.; Freishtat, R. J.; Anas, N.; Meyer, K.; et al. The Pediatric Sepsis Biomarker Risk Model. *Critical Care* **2011**, *16*, No. R174.
22. Bozza, F. A.; Salluh, J. I.; Japiassu, A. M.; Soares, M.; Assis, E. F.; Gomes, R. N.; Bozza, M. T.; Castro-Faria-Neto, H. C.; Bozza, P. T. Cytokine Profiles as Markers of Disease Severity in Sepsis: A Multiplex Analysis. *Critical Care* **2007**, *11* No. R49.
23. Endo, T.; Kerman, K.; Nagatani, N.; Hiepa, H. M.; Kim, D. K.; Yonezawa, Y.; Nakano, K.; Tamiya, E. Multiple Label-Free Detection of Antigen-Antibody Reaction using Localized Surface Plasmon Resonance-Based Core-Shell Structured Nanoparticle Layer Nanochip. *Anal. Chem.* **2006**, *78*, 6465–6475.
24. Ament, I.; Prasad, J.; Henkel, A.; Schmachtel, S.; Sonnichsen, C. Single Unlabeled Protein Detection on Individual Plasmonic Nanoparticles. *Nano Lett.* **2012**, *12*, 1092–1095.
25. Ahijado-Guzman, R.; Prasad, J.; Rosman, C.; Henkel, A.; Tome, L.; Schneider, D.; Rivas, G.; Sonnichsen, C. Plasmonic Nanosensors for Simultaneous Quantification of Multiple Protein–Protein Binding Affinities. *Nano Lett.* **2014**, *14*, 5528–5532.
26. Dahlin, A. B. Size Matters: Problems and Advantages Associated with Highly Miniaturized Sensors. *Sensors* **2012**, *12*, 3018–3036.
27. Ruemmele, J. A.; Hall, W. P.; Ruvuna, L. K.; Van Duyne, R. P. A Localized Surface Plasmon Resonance Imaging Instrument for Multiplexed Biosensing. *Anal. Chem.* **2013**, *85*, 4560–4566.
28. Bhagawati, M.; You, C.; Piehler, J. Quantitative Real-time Imaging of Protein-Protein Interactions by LSPR Detection with Micropatterned Gold Nanoparticles. *Anal. Chem.* **2013**, *85*, 9564–9571.
29. Nusz, G. J.; Curry, A. C.; Marinakos, S. M.; Wax, A.; Chilkoti, A. Rational Selection of Gold Nanorod Geometry for Label-Free Plasmonic Biosensors. *ACS Nano* **2009**, *3*, 795–806.
30. Haes, A. J.; Zou, S. L.; Schatz, G. C.; Van Duyne, R. P. Nanoscale Optical Biosensor: Short Range Distance Dependence of the Localized Surface Plasmon Resonance of Noble Metal Nanoparticles. *J. Phys. Chem. B* **2004**, *108*, 6961–6968.
31. Cao, J.; Sun, T.; Grattan, K. T. V. Gold Nanorod-Based Localized Surface Plasmon Resonance Biosensors: A Review. *Sens. Actuators, B* **2014**, *195*, 332–351.
32. Ikami, M.; Kawakami, A.; Kakuta, M.; Okamoto, Y.; Kaji, N.; Tokeshi, M.; Baba, Y. Immuno-Pillar Chip: A New Platform for Rapid and Easy-to-Use Immunoassay. *Lab Chip* **2010**, *10*, 3335–3340.
33. *Guidance for Industry: Bioanalytical Method Validation*; Food and Drug Administration, U.S. Department of Health and Human Services: Rockville, MD, 2001.
34. Agus, M. S. D.; Steil, G. M.; Wypij, D.; Costello, J. M.; Laussen, P. C.; Langer, M.; Alexander, J. L.; Scoppettuolo, L. A.; Pigula, F. A.; Charpie, J. R.; et al. Tight Glycemic Control *versus* Standard Care after Pediatric Cardiac Surgery. *N. Engl. J. Med.* **2012**, *367*, 1208–1219.
35. Mahle, W. T.; Matthews, E.; Kanter, K. R.; Kogon, B. E.; Hamrick, S. E.; Strickland, M. J. Inflammatory Response after Neonatal Cardiac Surgery and Its Relationship to Clinical Outcomes. *Ann. Thorac. Surg.* **2014**, *97*, 950–6.
36. Ashraf, S. S.; Tian, Y.; Zacharrias, S.; Cowan, D.; Martin, P.; Watterson, K. Effects of Cardiopulmonary Bypass on Neonatal and Paediatric Inflammatory Profiles. *Eur. J. Pediatr. Surg.* **1997**, *12*, 862–868.
37. Seghaye, M. C.; Duchateau, J.; Bruniaux, J.; Demontoux, S.; Bosson, C.; Serraf, A.; Lecronier, G.; Mokhfi, E.; Planche, C. Interleukin-10 Release Related to Cardiopulmonary Bypass in Infants undergoing Cardiac Operations. *J. Thorac. Cardiovasc. Surg.* **1996**, *111*, 545–553.